Bibliography

[1] S. Covrig, E08-014 Cryogenic Target System Simulation, 2013.

[2] L. L. Frankfurt, M. I. Strikman, D. B. Day, and M. Sargsyan, Phys. Rev. C **48**, 2451 (1993).

[3] CLAS Collaboration, K. S. Egiyan *et al.*, Phys. Rev. Lett. **96**, 082501 (2006).

[4] N. Fomin *et al.*, Phys. Rev. Lett. **108**, 092502 (2012).

[5] D. Meekins, E08-014 target report, `http://hallaweb.jlab.org/experiment/E08-014/analysis/HallA_Target_Configuration_Apr2011.pdf`, 2011.

Chapter 1

Non-Uniform Cryogenic Targets

As discussed in Section 5.4.2, all cryogenic targets (cryo-targets) present strange distributions of z_{react}, which indicate that their densities were not uniform but instead, vary along the 20 cm cells. As proved by a Monte Carlo simulation of the cryogenic target system [1], such non-uniform density profiles were because of the special target cell design and the direction of the cryogenic flow, as shown in Fig. 1.1.

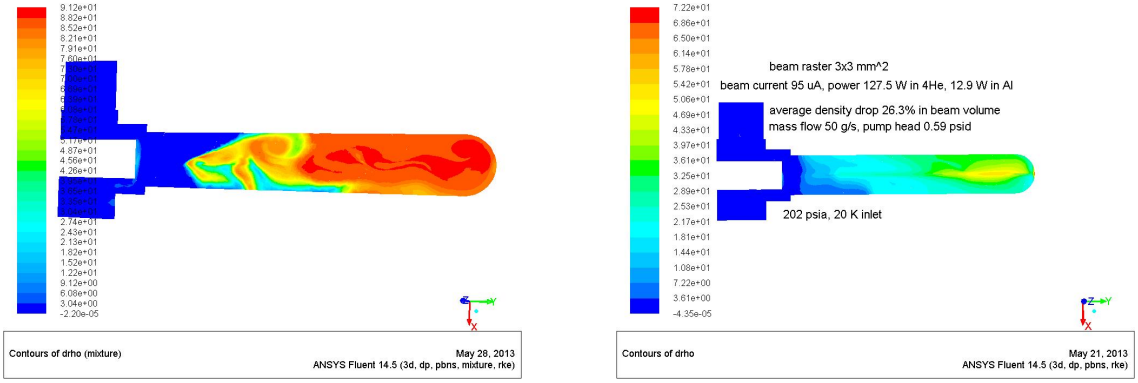

(a) ^2H (b) ^4He

Figure 1.1: Cryo-target density profiles from simulation.

Extracting cross sections of electron scattering on a target requires the accurate value of target luminosity, which depends on the beam current because of the boiling effect. While the boiling effect for a solid target is negligible, for these non-uniform cryo-targets, the boiling effect should be significant and have to be evaluated independently at different location along the target cells. Meanwhile, the radiation correction becomes more complicated since the radiation effect largely depends on the location and direction of the electron-scattering process. In this chapter, a detailed study of the boiling effect is given, followed by an discussion of extracting the cry-target density distributions. A procedure to evaluate the radiation correction factors for non-uniform cryo-targets will be introduced at the end.

1.1 Boiling Study

During E08-014, several boiling study runs were taken at different current values for three cryo-targets, as well as ^{12}C target, which was used to check any rate-dependence effects which can alter the boiling study results.

The experimental yield depends on the target density, the beam charge and the cross section of electron-nucleus scattering. While the average cross section shouldn't change for one kinematic setting, the yield normalized by the beam charge should be directly proportional to the target density. By fitting the change of the yield as a function of current, one can obtain the variation of the target density at different current, given as:

$$Y(I) = Y(0) + Slop \cdot I \longrightarrow \rho(I) = \rho(0) \cdot (1.0 + BF \cdot I/100), \tag{1.1}$$

where $BF = Y(0)/Slop$ is the boiling factor of the target. The variation of the yields with currents is described by a linear function which will be proved to be a valid assumption. $Y(I)$, the yield for one run with beam current I, is the total number of experimental events after all necessary cuts divided by the the total accumulated charge. $Y(0)$ is the yield extrapolated to zero beam current. Fig. 1.2 gives the fitting result of ^{12}C which indicates that for a fixed target density, the yield does not change at different current.

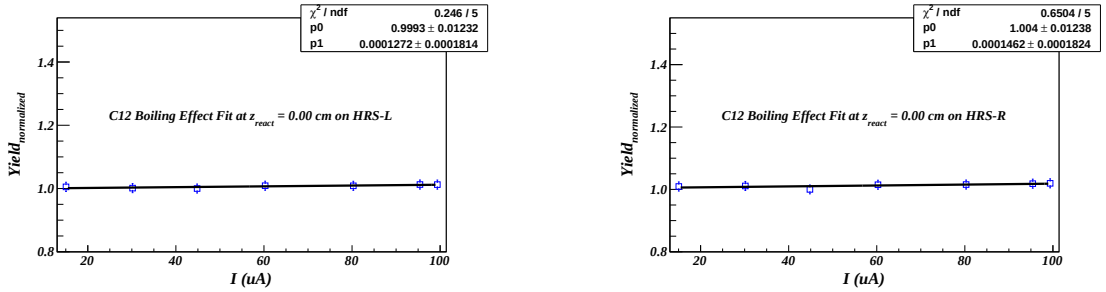

(a) ^{12}C on HRS-L (b) ^{12}C on HRS-R

Figure 1.2: ^{12}C boiling effect fitting. Since ^{12}C should have very small boiling effect, this study is used to check any rate-dependence effect at different current settings

For cryo-target, the data was binned in z_{react} which was divided into 60 bins. In each bin, the yield was calculated and one can fit the boiling factor by the formula:

$$Y(I, z^i_{react}) = Y(0, z^i_{react}) + Slop(z^i_{react}) \cdot I, , \quad where\ i = 1, \cdots, 60, \tag{1.2}$$

and,

$$\rho(I, z^i_{react}) = \rho(0, z^i_{react}) \cdot (1.0 + BF(z^i_{react}) \cdot I/100), \tag{1.3}$$

where,

$$BF(z^i_{react}) = \frac{Y(0, z^i_{react})}{Slop(z^i_{react})}. \tag{1.4}$$

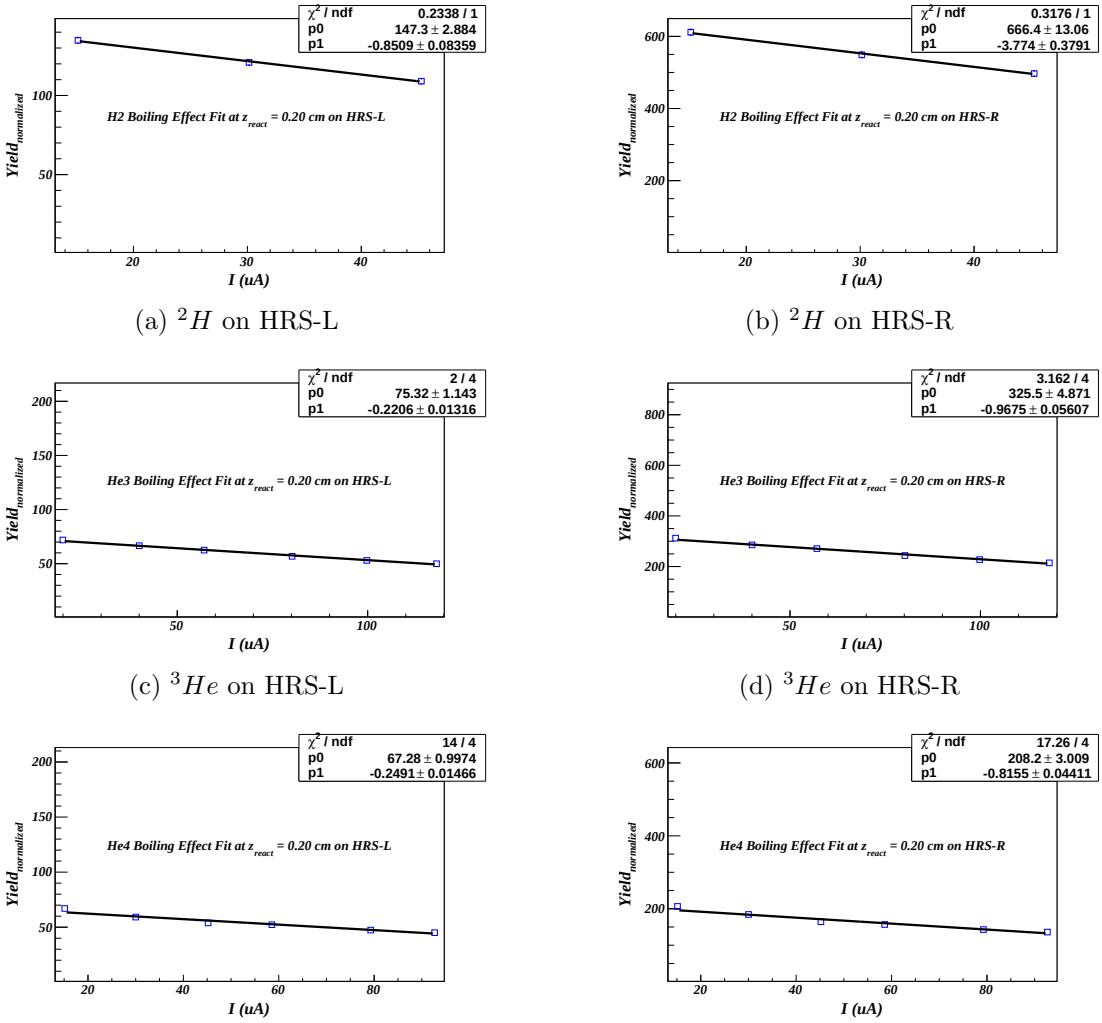

(a) ^2H on HRS-L (b) ^2H on HRS-R

(c) ^3He on HRS-L (d) ^3He on HRS-R

(e) ^4He on HRS-L (f) ^4He on HRS-R

Figure 1.3: Cryo-targets boiling effect fitting. They are examples near the center of the targets. Each target was divided into 60 bins along the target cell, where the boiling factor was individually fitted.

During the fitting, the values of yields have been normalized to their minimum values since the absolute values are irrelevant.

As examples, Fig. 1.3 shows the fitting results of boiling factors at the center of z_{react} for three cryo-targets, where the curves are well fitted by linear functions. The curve of normalized $Y(0, z^i_{react})$ denotes the target density profile along the cell, as shown in Fig. 1.4, where the peaks of end-cups are clearly presented. The distribution of $BF(z^i_{react})$ for each target, given in Fig. 1.5, shows the boiling effect at different z_{react}, and demonstrates that the non-uniform cryo-target densities were mainly because of the highly localized boiling effects. In the plot the values of z_{react} at the positions of end-cups are close to zero which agree with the fact that the density of aluminium walls shouldn't change with beam current. Results from both HRSs were

compared and agree nicely with each other.

1.2 Extracting Density Distributions

From Eq (1.2), the target density profile can be obtained by extracting the distribution of $Y(0)$ during the boiling study. In this section, a different method is applied to extract the density distribution by using the experimental data and simulation data.

Since z_{react} is along the incoming beam direction which is also the orientation of the target cell, the z_{react} distribution in the experimental data, z^{EX}_{react}, gives the distribution of yields in a certain current setting, which also corresponds to the variation of density along the target. However, z^{EX}_{react} should also contain the acceptance effect of the HRS and the cross section effect, which statistically weights the yields in different z_{react} location where the central scattering angle varies. One can apply the simulation data generated by SAMC, which simulates the acceptance effect of HRSs, to plot the simulated z_{react} distribution,z^{MC}_{react}, which is furthered weighted by the cross section values calculated from XEMC. When the target density distribution in the simulation data is uniform, z^{MC}_{react} only carries the acceptance effect and the cross section effect. By plotting the histograms of z^{EX}_{react} and z^{MC}_{react} with the same range and bin-size, one takes to ratio of two histogram, which leads to a clean relative density distribution of the target at the current setting.

The plots on the left hand side of Fig. 1.6 show the distribution of z^{EX}_{react} and z^{MC}_{react} at three different current settings for each target, while the plots on the right hand side give the fitting results of the relative density distributions. A polynomial function is used for each fitting process.

One can use the density distributions at the minimum current (15 uA, 20 uA and 15 uA for ^2H, ^3He and ^4He, respectively), and apply the boiling factors to calculate the density distribution at beam current equal to zero, $\rho(0)$. Then the density distribution at any current settings, $\rho_{Calc}(I)$ can be calculated using Eq (1.3). To verify the boiling study results and the density distributions at different current settings, the distributions of $\rho_{Calc}(I)$ and $\rho(I)$ extracted in Fig. 1.6 were compared, as shown in Fig. 1.7. Note that the contribution from the two end-cups were removed by applying the cut, $|z_{react}| \leq 7.5\ cm$. The plots reveal that the results of boiling study successfully characterize the change of target density with different beam current.

Fig. 1.7 also compares the distributions of the target density obtained from the boiling study and from the method discussed in this section. Ignoring the statistically fluctuation of the histograms, both methods give similar density profiles, and the small difference can be explained by the errors of the HRS acceptance simulation in SAMC and the cross section model in XEMC.

1.3 Absolute Density

When the density distribution is uniform, the absolute density of a cry-target can be calculated using the temperature and pressure readings from the target system with the fixed volume of the target cell. However, the calculation becomes impossible when the density is not uniform since the temperature and pressure fluctuate inside the target. While the relative density distribution has been extracted as discussed in previous section, one can obtain the absolute density distribution by calculating the density at the entrance of the target cell where the temperature and pressure were monitored.

Whereas, the extracted relative density distribution at the entrance does not reflect the true density profile of the cryo-target due to the contamination of the aluminium end-cup during the boiling study, and an assumption has been made to assign the density value at the entrance to the value at $-10 \leq z_{react} \leq -7.5\ cm$. The true value should not deviate too far away from this value since this location is very close to the entrance and the coolant flow should be able to maintain the same temperature as at the entrance. The deviation can be corrected when comparing the experimental yield and the simulation yield, while the last one, yet, depends on the cross section model. To obtain the accurate density, one can utilize the 2N-SRC plateaus of cross section ratio of the carbon target to the cryo-targets [2–4], which have been well measured in previous experiments. Table 1.1 gives the densities of cryo-targets at the entrance and the yield-normalized density at $z_{react} = 7.5\ cm$, where the values will be updated when they are further normalized by the 2N-SRC plateaus.

Target:	^2H	^3He-I	^3He-II	^4He
$\rho_{entrance}$ (g/cm^3):	0.1676	0.0213	0.0296	0.0324
$\rho_{z_{react}=-7.5\ cm}$ (g/cm^3):	0.1906	0.0210	0.0292	0.0280

Table 1.1: Cryo-targets densities, where two values of the ^3He density refer to two different run periods. The values of $\rho_{entrance}$ are calculated from the temperature and pressure reading [5]. The values of $\rho_{z_{react}=-7.5\ cm}$ are the values of $\rho_{entrance}$ normalized by the ratio of the experimental yield and the simulation yield and will be further corrected by comparing the 2N-SRC plateaus.

1.4 Radiative Correction

The most essential parameter during the radiative correction is the radiation length of the target. For uniform target, the radiation length is usually evaluated at the center of the target. For non-uniform targets, such an approximation has to be carefully examined.

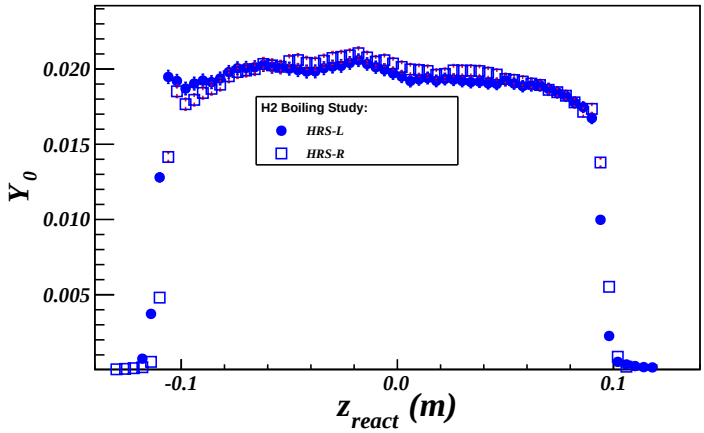

(a) $^2H2$

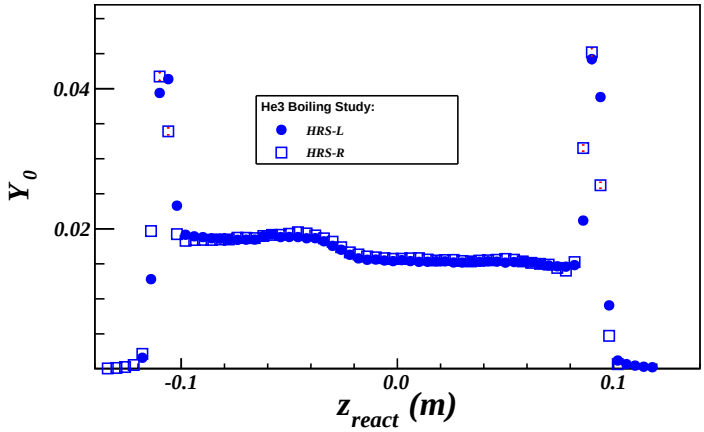

(b) ^3He

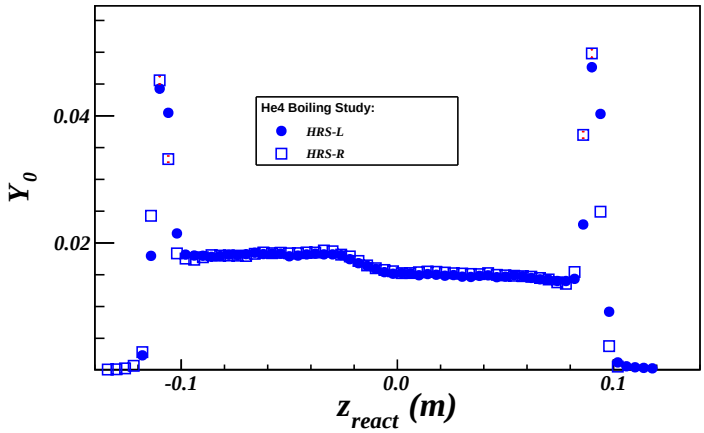

(c) ^4He

Figure 1.4: Cryo-target density profiles from boiling study. The results from both HRSs agree with each other for each target, and the peaks denote the contributions from the end-cups of the target cell.

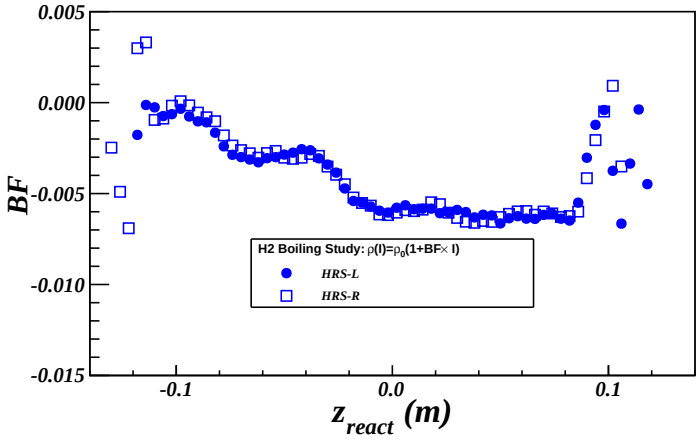

(a) $^2H2$

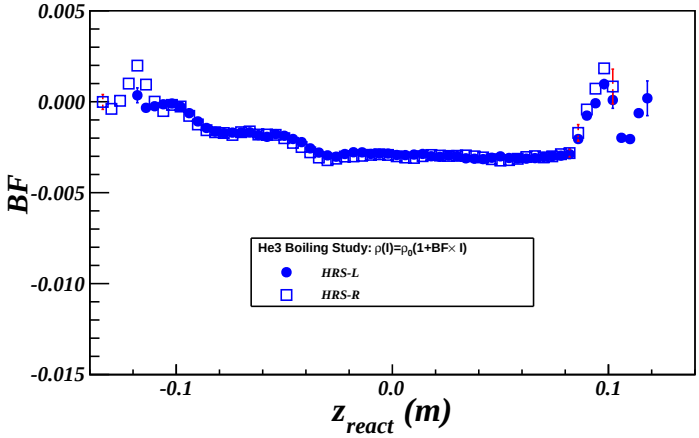

(b) ^3He

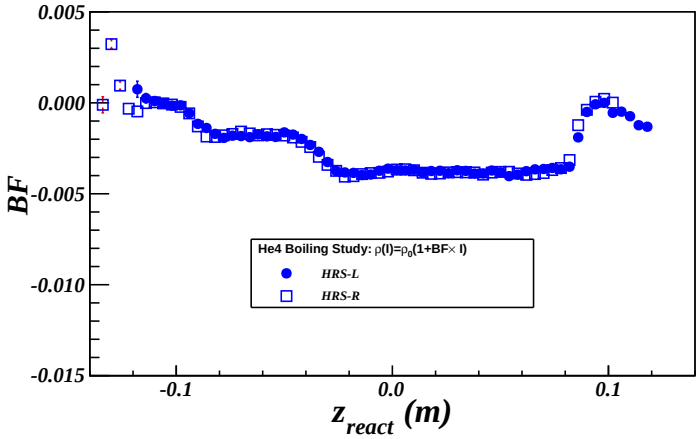

(c) ^4He

Figure 1.5: Cryo-target boiling factor distribution. Each plot clearly shows that the boiling effect varies along the target cells. The boiling factors at the end-cups are reasonably close to zero. The studies from both HRSs give consistent results.

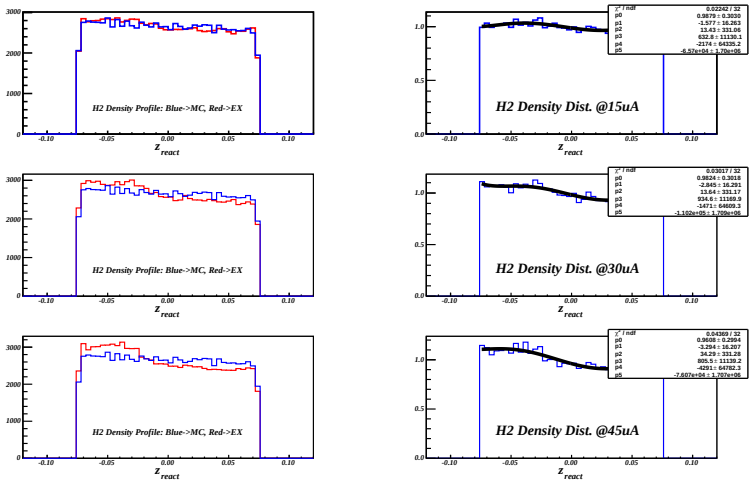

(a) $^2H2$

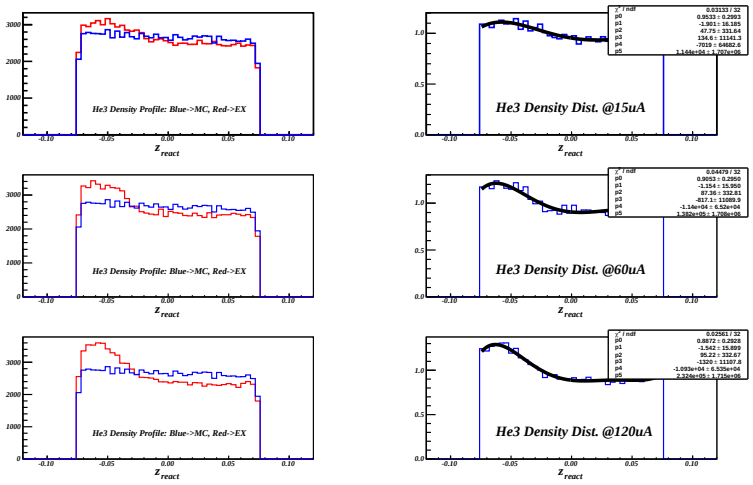

(b) ^3He

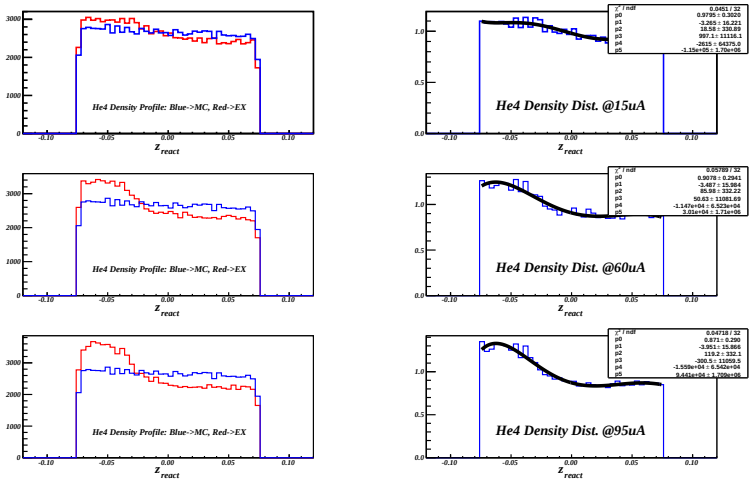

(c) ^4He

Figure 1.6: Cryo-target density distributions extracted from data. The density distribution was extracted by taking the histogram ratio of z_{react} from experimental data (red lines in plots on the right panel) and from simulation data with flat density distribution (blue lines in plots on the right panel). For each target, the density distributions at the minimum, middle and maximum currents were individually extracted (on left panel). The current settings are given in the plots.

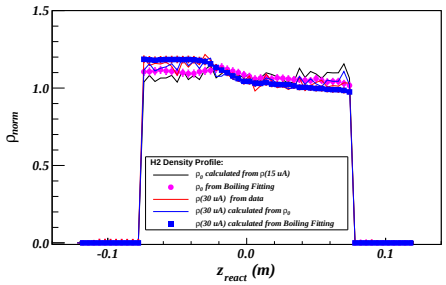

(a) ^2H at I=30 uA

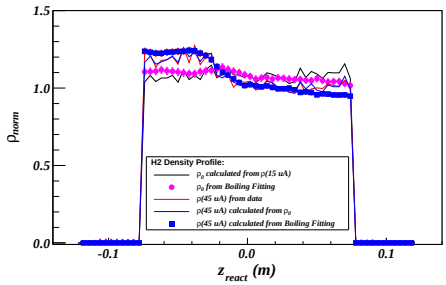

(b) ^2H at I=45 uA

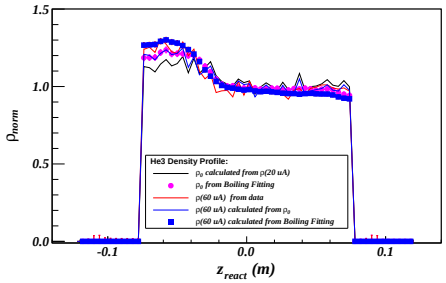

(c) ^3He at I=60 uA

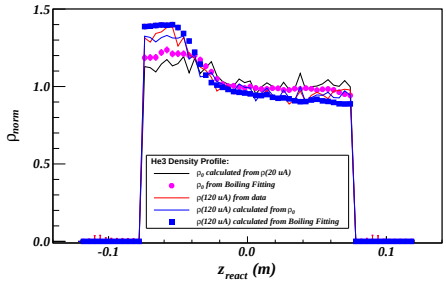

(d) ^3He at I=120 uA

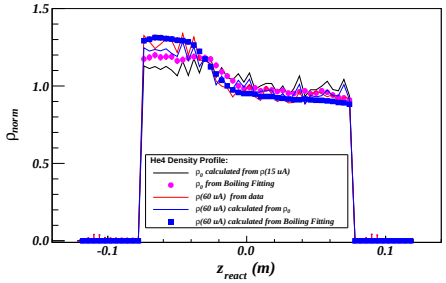

(e) ^4He at I=60 uA

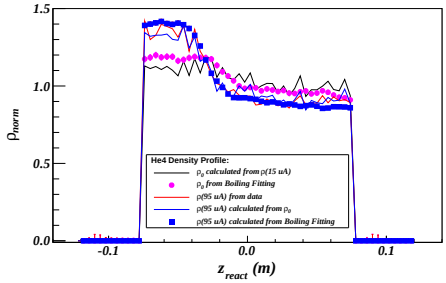

(f) ^4He at I=95 uA

Figure 1.7: Cryo-targets relative density distribution extracted from data and corrected by the boiling factors. The density values were calculated in each z_{react} bin and the peaks in these distribution were due to the statistical fluctuation. To remove the contribution of the end-cups, a cut was apply on the target length, $|z_{react}| \leq 7.5\ cm$